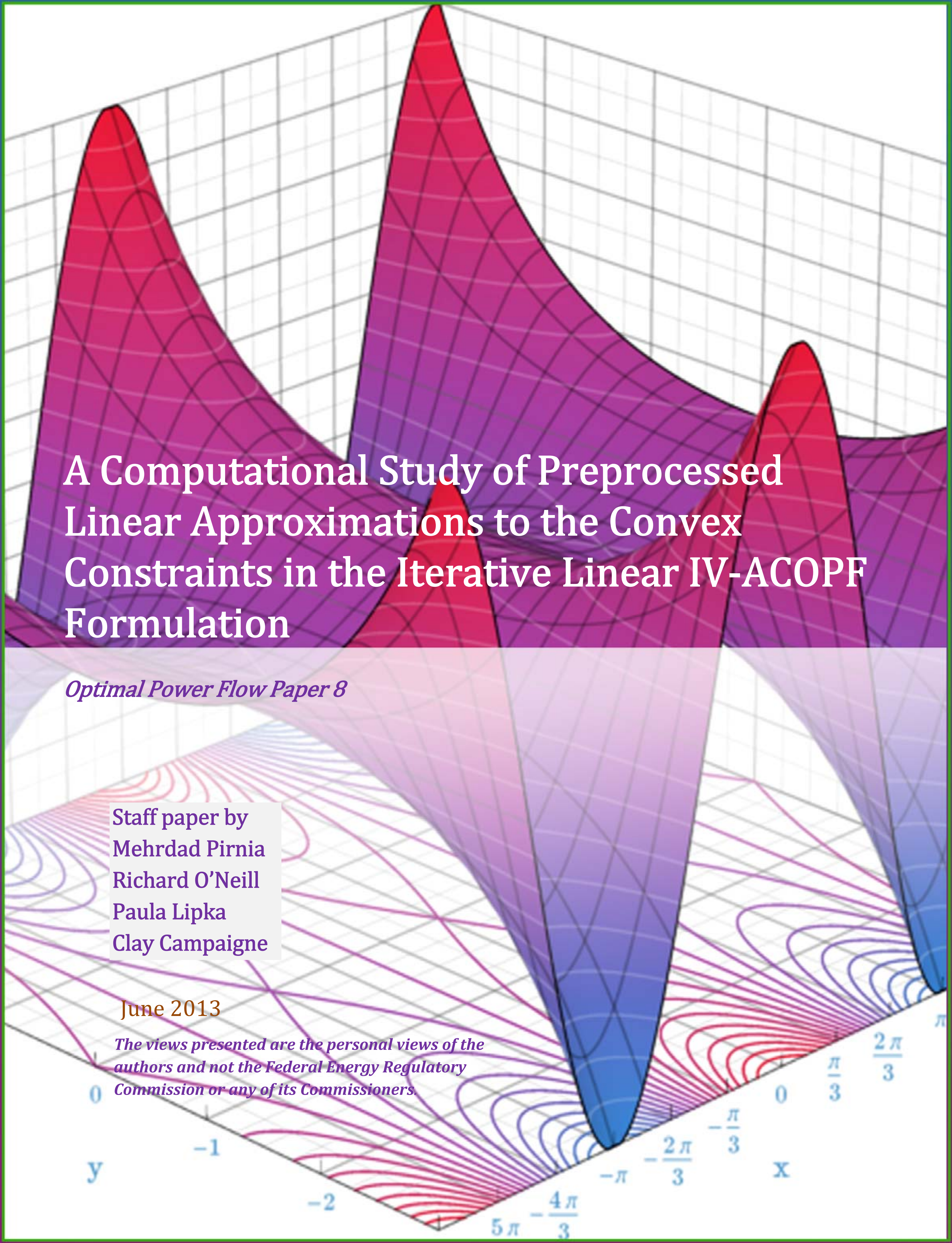

A Computational Study of Preprocessed Linear Approximations to the Convex Constraints in the Iterative Linear IV-ACOPF Formulation

Optimal Power Flow Paper 8

Staff paper by
Mehrdad Pirnia
Richard O'Neill
Paula Lipka
Clay Campaigne

June 2013

The views presented are the personal views of the authors and not the Federal Energy Regulatory Commission or any of its Commissioners.

A Computational Study of Linear Approximations to the Convex Constraints in the Iterative Linear IV-ACOPF Formulation

Mehrdad Pirnia, Richard O'Neill, Paula Lipka, Clay Campaigne
mpirnia@uwaterloo.ca; richard.oneill@ferc.gov; plipka@berkeley.edu;
claycampaigne@bekeley.edu
June 2013

Abstract and Executive Summary

In this paper, we test the effect of preprocessed and iterative linear cuts on the convex constraints (maximum voltage and maximum current) in iterative linear approximation of the current voltage (IV) formulation of the ACOPF (ILIV-ACOPF) problem. The nonconvex constraints are linearized using iterative first order Taylor series approximation. The ILIV-ACOPF is solved as a single linear program or a sequence of linear programs. The ILIV-ACOPF model is tested on the 14-bus, 30-bus, 57-bus and 118-bus IEEE test systems. The execution time and the quality of the solution obtained from the ILIV-ACOPF are compared for different test systems and benchmarked against the equivalent nonlinear ACOPF formulation. The results show execution time up to 8 times faster and solutions close to the nonlinear solver. The performance of different algorithmic parameters varies depending on the test problem. As the number of preprocessed cuts for each bus and line increases, the relative error decreases. The results indicate that 16 to 32 constraints are the best number of preprocessed constraints in a tradeoff between accuracy and solution time. The marginal value of more than 32 and maybe 16 preprocessed constraints in this setting is negative. Nevertheless, the number of preprocessed constraints can be set based on the performance and requirements of the specific problem being solved. Using iterative cuts often results in faster convergence to a feasible solution. When solving without using iterative cuts, the solution is within 18% of the best-known nonlinear feasible solution; with iterative cuts, the solution is within 2.5% of the best-known nonlinear solution. At 16 or 32 preprocessed constraints, solution time is up to about 8 times faster than the nonlinear solver (IPOPT).

Table of Contents

1. Introduction

Since Carpentier (1962) introduced AC optimal power flow (ACOPF) problem, the ACOPF has received considerable attention. It is at the heart of power system efficiency. The ACOPF optimizes the steady state performance of an AC power system by minimizing an objective function such as generation cost or maximizing market surplus while satisfying system constraints including nodal real power balance, nodal reactive power balance, bounds on bus voltages, bounds on transmission lines flow, bounds on real and reactive power injections, and system contingencies. Since the ACOPF's introduction, different objective functions and formulations have been tried (see Cain et al). The canonical ACOPF problem uses real and reactive power injections and the polar representation of voltage for the network equations. ACOPF problems have nonconvex continuous functions and can be large. More difficult variations include binary variables for topology control and unit commitment (see, for example, Potluri and Hedman).

Solving an ACOPF problem that meets power system's physical criteria has continued to be a challenge in power system operations. While most NLP solvers find local optimal solutions most of the time, their lengthy solution times and poor convergence (especially with the introduction of binary variables) have focused attention on linear approximations. Linear programming (LP) methods play a significant role in solving these problems with more robust solutions and better execution times. One common linear program approach is the distribution factor model. In another linear program approach, the real part of the admittance matrix is considered negligible, reactive power and voltage magnitude are dropped from the formulation, and bus voltage angles are assumed to be near-zero (Stott, et al., 2009).

A vast body of literature proposes different optimization methods to solve the ACOPF including Lagrangian approaches, sequential quadratic programming, sequential linear programming, interior point methods, and heuristics. Literature reviews appear periodically (see, for example, Dommel and Tinney, Huneault and Galiana, Momoh, et al, Frank and Steponavice and Castillo and O'Neill, 2013a). The literature reviews present an evolution of approaches to solve the ACOPF. Capitanescu et al (2011) reviews the state of the art and challenges to the optimal power flow computations including corrective post-contingency actions, voltage and transient stability constraints, problem size reduction, discrete variables and uncertainty.

O'Neill el al (2012a) formulate the ACOPF in several ways, compare each formulation's properties, and argue that the rectangular current-voltage or "IV" formulation and its linear approximations may be easier to solve than the traditional quadratic power flow "PQV" formulation. O'Neill et al (2012b) compare solving the IV linear approximation of the ACOPF to solving the ACOPF with several nonlinear solvers. In general, the linear approximation approach is more robust and faster than several of the commercial nonlinear solvers. On several starting points, the nonlinear solvers failed to converge or contained positive relaxation variables above the threshold. The iterative linear program approach finds a near-feasible near-optimal in almost all problems and starting points. Castillo and O'Neill (2013b) present an experimental framework, statistical methods and numerical results from testing commercial nonlinear solvers with several ACOPF formulations and initializations. The experiments indicate a clear advantage to employing a rectangular formulation over a polar formulation and using multiple solvers.

In spite of all the work that has been done, the ACOPF remains 'very much a work in progress' (Stott and Alsaç, 2012). Further, they state that solutions to the problems encountered in 'real-life' are 'not easy to obtain' and still require significant individual intervention and tuning.

In this paper, we test the iterative linearization (IL) approach to the IV ACOPF formulation, proposed in (O'Neill, et al., 2012) on four IEEE standard test problems (14-bus, 30-bus, 57-bus and 118-bus test systems) with line current constraints added. We vary the number of preprocessed linear cuts, to approximate the convex quadratic voltage and current constraints with and without iterative constraints. We report the solution time and accuracy.

The rest of the paper is organized as follows. Section 2 presents the notation to be used in following sections. Section 3 presents a brief review of the IV-ACOPF and ILIV-ACOPF formulations. Section 4 presents and discusses the linear approximation techniques, such as pre-processed cuts, iterative cuts and non-convex constraint linearizations, which are used to approximate the IV-ACOPF formulation. Section 5 presents numerical results for the test systems showing the performance of this method compared to the nonlinear OPF problem. Finally, Section 6 highlights the main conclusions and contributions of the paper. The appendix contains the numerical results.

2. Notation

Indices and Sets

n, m are bus (node) indices; $n, m \in \{1, \ldots, N\}$ where N is the number of buses.

k is a transmission element. $k \in \{1, \ldots, K\}$ where K is the number of transmission elements. Each k has a pair of terminal buses n and m.

r real part of the complex number or variable (superscript)

j imaginary part of the complex number or variable (superscript)

$\boldsymbol{j}$ is $(-1)^{1/2}$

s is the index of the preprocessed constraints where $s \in S = \{0, 1, \ldots, S\text{-}1\}$.

h indexes a major iteration (solving a linear program) of the algorithm

Variables

p_n is the real power injection (positive) or withdrawal (negative) at bus n

q_n is the reactive power injection or withdrawal at bus n

v^r_n real part of the voltage at bus n

v^j_n imaginary part of the voltage at bus n

v_n is the voltage magnitude at bus n. $v_n = [(v^r_n)^2 + (v^j_n)^2]^{1/2}$

i^r_n real part of the current at bus n

i^j_n imaginary part of the current at bus n

i_n is the current magnitude at bus n where $i_n = [(i^r_n)^2 + (i^j_n)^2]^{1/2}$

i^r_{nmk} real part of the current from bus n to bus m on line k

i^j_{nmk} imaginary part of the current from bus n to bus m on line k

i_{nmk} is the current magnitude into k at bus n (to bus m); $i_{nmk} = [(i^r_{nmk})^2 + (i^j_{nmk})^2]^{1/2}$

V the complex vector of bus voltages; $V = V^r + \boldsymbol{j}V^j$

I the complex vector of bus current injections, $I = I^r + \boldsymbol{j}I^j$

P the vector of real power injections

Q the vector of reactive power injections

Parameters and Functions

$c^p{}_n(p_n)$	cost function of real power p_n at bus n
$c^q{}_n(q_n)$	cost function of reactive power q_n at bus n
$c^{pl}{}_n(p_n)$	linear cost function of real power p_n at bus n
$c^{ql}{}_n(q_n)$	linear cost function of reactive power q_n at bus n
b_{nmk}	imaginary part of the admittance matrix for k between bus n and m
g_{nmk}	real part of the admittance matrix for k between bus n and m
$p^{min}{}_n$	minimum required real power at bus n
$p^{max}{}_n$	maximum allowed real power at bus n
$q^{min}{}_n$	minimum required reactive power at bus n
$q^{max}{}_n$	maximum allowed reactive power at bus n
$v^{min}{}_n$	minimum required voltage magnitude at bus n
$v^{max}{}_n$	maximum allowed voltage magnitude at bus n
$\underline{v}^r{}_{nh}$	Coefficeint for real component of bus voltage cut at n from iteration h
$\underline{v}^j{}_{nh}$	Coefficeint for imaginary component of bus voltage cut at n from iteration h
$\underline{i}^r{}_{nh}$	real part of the current at bus n at the previous linear program solution
$\underline{i}^j{}_{nh}$	imaginary part of the current at bus n at the previous linear program solution
$i^{max}{}_{nmk}$	maximum allowed current magnitude on line k connecting bus n to bus m
$\underline{i}^r{}_{nmkh}$	coefficient of the real component of the line flow constraint on line k and iteration h
$\underline{i}^j{}_{nmkh}$	coefficient of the imaginary component of the line flow constraint on line k and iteration h

3. Formulations

In 2012, O'Neill et al (2012) introduced a linearization approach to the IV formulation. In the IV-ACOPF formulation, the network-wide nodal-balance constraints are linear in the current and voltage ($I = YV$), rather than the nonconvex power flow equations based on power and voltage ($S = VI^*$). The objective function is linearized using a step function approximation.

IV-ACOPF Formulation. The rectangular form of the nonlinear IV-ACOPF is shown below.

$$\text{Min} \quad \sum_n [c^{pl}{}_n(p_n) + c^{ql}{}_n(q_n)] \tag{1}$$

$$i^r{}_n = \sum_{mk} i^r{}_{nmk} \quad \text{for all } n \tag{2}$$

$$i^j{}_n = \sum_{mk} i^j{}_{nmk} \quad \text{for all } n \tag{3}$$

$$i^r{}_{nmk} = g_{nmk}(v^r{}_n - v^r{}_m) - b_{nmk}(v^j{}_n - v^j{}_m) \quad \text{for all } k \tag{4}$$

$$i^j{}_{nmk} = b_{nmk}(v^r{}_n - v^r{}_m) + g_{nmk}(v^j{}_n - v^j{}_m) \quad \text{for all } k \tag{5}$$

$$p_n = v^r{}_n i^r{}_n + v^j{}_n i^j{}_n \quad \text{for all } n \tag{6}$$

$$p_n \le p^{max}{}_n \quad \text{for all } n \tag{7}$$

$$p^{min}{}_n \le p_n \quad \text{for all } n \tag{8}$$

$$q_n = v^j{}_n i^r{}_n - v^r{}_n i^j{}_n \quad \text{for all } n \tag{9}$$

$$q_n \le q^{max}{}_n \quad \text{for all } n \tag{10}$$

$$q^{min}{}_n \le q_n \quad \text{for all } n \tag{11}$$

$$(v^r_n)^2 + (v^j_n)^2 \le (v^{max}_n)^2 \qquad \text{for all } n \qquad (12)$$

$$(v^{min}_n)^2 \le (v^r_n)^2 + (v^j_n)^2 \qquad \text{for all } n \qquad (13)$$

$$(i^r_{nmk})^2 + (i^j_{nmk})^2 \le (i^{max}_{nmk})^2 \qquad \text{for all } k \qquad (14)$$

The above IV-ACOPF formulation has $6N$ variables as $(P, Q, V^r, V^j, I^r, I^j)$. As shown in (2) - (5), the current flow equations are linear. These equations replace the quadratic or trigonometric forms of the power flow equations (rectangular and polar forms) in traditional ACOPF models. In this formulation, real power equation (6) and reactive power equation (9) are quadratic nonconvex functions of current and voltage with bounds (7), (8), (10), and (11). Maximum bus voltage magnitude and current flow limits (12) and (14) are quadratic convex constraints. The minimum voltage magnitude constraint is a nonconvex quadratic constraint (13).

4. Linear Approximations

Iterative Linear Current Voltage (ILIV)-ACOPF. To form the ILIV-ACOPF from the above ACOPF problem, we replace the convex constraints with strong linear cuts. Strong cuts are hyperplanes that are tangent to the constraint sets and contain the constraints. These linear constraints form a linear relaxation (outer approximation) of nonlinear convex constraints. The nonconvex constraints are approximated by first order Taylor's series approximations.

Pre-processed cuts. Preprocessed cuts on the current and voltage maximum magnitude constraints are put into the model at the first step. The strong iterative cuts at each major iteration are added when a linear program solution violates a nonlinear convex constraint. These cuts are added and kept until the convergence criteria is satisfied.

The maximum voltage and current magnitude constraints (12) and (14) form a circle with its interior, generically, $x^2 + y^2 \le r^2$. We add strong linear cuts to create a circumscribing polygon, as shown in Figure 1. For any angle $\underline{\theta}$, let $\underline{x} = r\cos\underline{\theta}$ and $\underline{y} = r\sin\underline{\theta}$. Since $(r\cos\underline{\theta})^2 + (r\sin\underline{\theta})^2 = r^2$, $(\underline{x}, \underline{y})$ is a point on the circle and $\underline{x}x + \underline{y}y \le r^2$ is a strong cut for any $\underline{\theta}$.

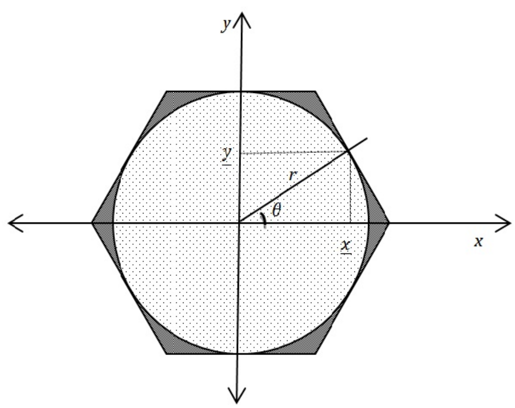

Figure 1: Polygon circumscribing a circle

Now, let $\underline{\theta}_s = 2\pi/s$, $\underline{x}_s = r\cos(\underline{\theta}_s)$ and $\underline{y}_s = r\sin(\underline{\theta}_s)$ where $s \in \{1, \ldots, S\} = \mathcal{S}$. The constraint set defined by $\mathcal{S}$ is a regular polygon, the maximum constraint violation of the circle is the distance from a vertex of the polygon, x, to the radius r, where $x = r/\cos(2\pi/S)$. The maximum relative error of the polygon is $x/r = 1/\cos(2\pi/S)$ as s increases $\cos(2\pi/S)$ approaches 1. Table 1 shows x/r when $S = 4$, 8, 16, 32 and 64 are used to approximate the circle. For example, increasing the cuts from 4 to 16 cuts increases the ratio x/r from 1.41 to 1.02. Adding 32 cuts provides a close approximation to the actual feasible area of the convex constraints.

Table 1:Maximum relative error

Number of linear cuts	Angle in radians (π/n)	Cos (angle)	1/ Cos (angle)
4	0.785	0.707	1.414
8	0.393	0.924	1.082
16	0.196	0.981	1.020
32	0.098	0.995	1.005
64	0.049	0.999	1.001

Iterative cuts. Let x_h, y_h be a solution at the major iteration h. If x_h, y_h violates a maximum magnitude constraint, that is, $z_h^2 = x_h^2 + y_h^2 > r^2$. Let $a = r/z_h$, $\underline{x} = ax_h$ and $\underline{y} = ay_h$, then

$$\underline{x}^2 + \underline{y}^2 = (ax_h)^2 + (ay_h)^2 = a^2(x_h^2 + y_h^2) = a^2(z_h^2) = r^2$$

For voltage constraints, $\underline{x}, \underline{y}$ and r are replaced with $\underline{v}^r_{nh}, \underline{v}^j_{nh}$ and v^{max}_n. For the current constraints x, y and r are replaced with $\underline{i}^r_{nmh}, i^r_{nmh}$ and i^{max}_{nmk}. These new iterative constraints reduce the feasible area and make the current optimal solution infeasible. At each iteration, the iterative constraints are added:

$$\underline{v}^r_{nh}\, v^r_n + \underline{v}^j_{nh}\, v^j_n \leq (v^{max}_n)^2$$

$$\underline{i}^r_{nmkh}\, i^r_{nmk} + \underline{i}^j_{nmkh}\, i^j_{nmk} \leq (i^{max}_{nmk})^2$$

The minimum voltage constraint is addressed by an active set approach, that is, it is only activated when the constraint is violated.

Nonconvex constraint linearization. The nonconvex constraint approximation is a first order Taylor series approximation and is updated at each major iteration. The minimum voltage constraint is addressed by an active set approach.

Using the pre-processed iterative cuts and first order Taylor series approximation the linear problem at major iteration h is:

LP_h	$= \text{Min} \sum_n [c^{pl}_n(p_n) + c^{ql}_n(q_n)]$		(15)
	$i^r_n = \sum_{mk} i^r_{nmk}$	for all n	(16)
	$i^j_n = \sum_{mk} i^j_{nmk}$	for all n	(17)
	$i^r_{nmk} = g_{nmk}(v^r_n - v^r_m) - b_{nmk}(v^j_n - v^j_m)$	for all k	(18)
	$i^j_{nmk} = b_{nmk}(v^r_n - v^r_m) + g_{nmk}(v^j_n - v^j_m)$	for all k	(19)
	$p_n = \underline{v}^r_{nh} i^r_n + \underline{v}^j_{nh} i^j_n + v^r_n \underline{i}^r_{nh} + v^j_n \underline{i}^j_{nh} - \underline{v}^r_{nh} \underline{i}^r_{nh} - \underline{v}^j_{nh} \underline{i}^j_{nh}$	for all n	(20)
	$p_n \leq p^{max}_n$	for all n	(21)
	$p^{min}_n \leq p_n$	for all n	(22)
	$q_n = \underline{v}^j_{nh} i^r_n - \underline{v}^r_{nh} i^j_n + v^j_n \underline{i}^r_{nh} - v^r_n \underline{i}^j_{nh} - \underline{v}^j_{nh} \underline{i}^r_{nh} + \underline{v}^r_{nh} \underline{i}^j_{nh}$	for h and all n	(23)
	$q_n \leq q^{max}_n$	for all n	(24)
	$q^{min}_n \leq q_n$	for all n	(25)
	$\cos\underline{\theta}_s v^r_n + \sin\underline{\theta}_s v^j_n \leq v^{max}_n$	for all n, s	(26)

$$\underline{v}^r_{nh}\, v^r_n + \underline{v}^j_{nh}\, v^j_n \le (v^{max}_n)^2 \qquad \text{for all } n, h \qquad (27)$$

$$\cos\underline{\theta}_s\, i^r_{nmk} + \sin\underline{\theta}_s\, i^j_{nmk} \le i^{max}_{nmk} \qquad \text{for all } k, s \qquad (28)$$

$$\underline{i}^r_{nmkh}\, i^r_{nmk} + \underline{i}^j_{nmkh}\, i^j_{nmk} \le (i^{max}_{nmk})^2 \qquad \text{for all } k, h \qquad (29)$$

Equations (15)-(19), (21), (22), (24) and (25) are the same in both formulations. Equations (26) and (28) are the preprocessed cuts. The minimum and maximum limits for real and reactive power are linearized at each iteration using first order Taylor series approximation in (20) and (23). Finally a new voltage and current cut for each infeasibility in (27) and (29) are added in each iteration.

The linearized procedure to solve the above ACOPF problem is:

1. Initialization: set $h = 0$ and $\underline{v}^r_{n0} = 1$, $\underline{v}^j_{n0} = 0$ for all buses n. Compute the starting values of i^r_{nmk} and i^j_{nmk} using equations (2) and (3). Calculate and add the preprocessed constraints.
2. Set $h = h+1$. Solve the above LP_h model.
3. Compute the real and reactive power magnitude using the nonlinear equations. Compute the voltage magnitude $v_{nh} = [(v^r_{nh})^2 + (v^j_{nh})^2]^{1/2}$. Calculate the average and maximum percent violation of the voltage, real power, and reactive power from their minimum and maximum limits. If the sum of the average percent violations of the voltage, real power, and reactive power is under a certain threshold, and the maximum violations of the nodal voltage, real power, and reactive power is also under a threshold, the solution is declared to be AC feasible. The solution process is stopped and the answer is returned. Otherwise continue.
4. The optimal values from this iteration are used to calculate the iterative cuts and the Taylor's series approximation as described above. Go to step 2.

Steps 2, 3 and 4 are called a major iteration.

5. Computational Results

We examine the performance of the ILIV-ACOPF problem with the preprocessed cuts and with iterative cuts (LP-IterIVCut) and without iterative cuts (LP-NoIterIVCut). The IEEE 14-bus, 30-bus, 57-bus and 118-bus test systems with tight and loose line current limits are used to test the performance of each procedure. Since the IEEE test problems have no generic line current limits, we used the approach in (Lipka, O'Neill and Oren, 2013) to establish the line current limits shown in Table 2. The results are then benchmarked against a nonlinear IV-ACOPF problem (NLP+LP Objective) with the same linear objective function as the linearized problem. For the 14-bus, 30-bus and 57-bus test systems, the convergence criteria for the sum of the average relative (to the bound) violations of the voltage, real power, and reactive power is under 0.005 and the sum of the maximum violations of the voltage, real power, and reactive power is under 0.001. However, because these tolerance levels cause convergence difficulty for the 118-bus system, they are changed to 0.05 and 0.01 respectively.

Table 2: Ratios used to calculate current limits and NLP objective value and Execution time

	14 Bus	30 Bus	57 Bus	118 Bus
Tight Constraint				
% of Maximum Optimal Current	18.5	93.3	76.2	24.3
Max Current Level	0.2264	0.3092	1.4027	0.9294
objective function value	107.4	6.092	432.2	1388.4
Execution time (sec)	1.12	5.23	20.28	87.59
Loose Constraint				
% of Maximum Optimal Current	51.1	95.4	77.0	71.9
Max Current Level	0.6246	0.3162	1.4168	2.7536
objective function value	86.51	5.973	425.5	1315.5
Execution time (sec)	0.89	5.81	30.92	70.72

The problems were solved on an Intel Xeon E7458 server with 8 64-bit 2.4GHz processors and 64 GB memory. The problems were formulated in GAMS (Rosenthal, et al., 2007). The nonlinear solver used was IPOPT version 3.8 (Waechter, 2007). The linear solver was GUROBI 5.0 (Rothberg, et al., 2010).

In the following sections, all results are normalized by the results from the IPOPT nonlinear solver to demonstrate a better comparison among the models and test problems. The actual values are in the appendix.

Effect of preprocessed cuts. As shown in figures 2-5, for both loose and tight current constraints, as the number of preprocessed cuts increases, the objective function value in most cases gets closer to the nonlinear objective function with iterative and without iterative cuts. However, as the number of preprocessed cuts increases beyond 32, the execution time increases and there is little, if any, improvement in the objective function value. The best performance measures for the execution time and the objective function value are obtained with 16 or 32 preprocessed cuts. For the 16 and 32 preprocessed cuts, in all but one case (14-bus test system with loose current limits and iterative cuts) the ILIV solves faster than the IPOPT. In most cases, the ILIV takes less than half the CPU time.

Effect of iterative cuts. Iterative cuts are important in improving the accuracy of the objective function value. In all cases, when the iterative cuts are implemented, the objective function value is significantly improved and is very close to the NLP objective function value. In addition, they can reduce the execution time, as the linear model converges much faster. For all the test systems the solution converged in less than 5 major iterations.

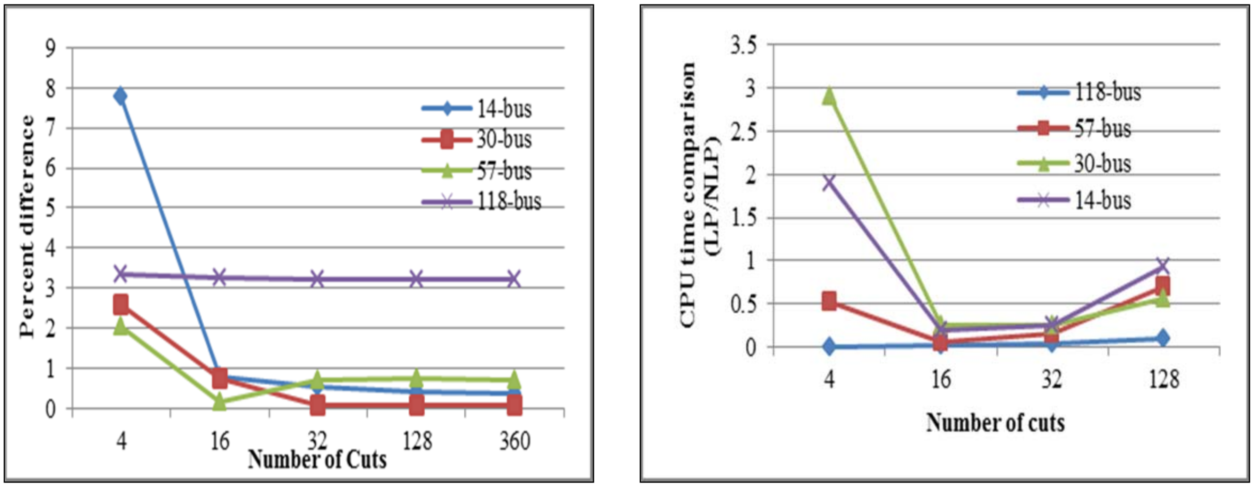

Figure 2. Objective Function Percent Difference and CPU Time Relative to the Nonlinear Solver for Loose Current Limit and No Iterative Cuts

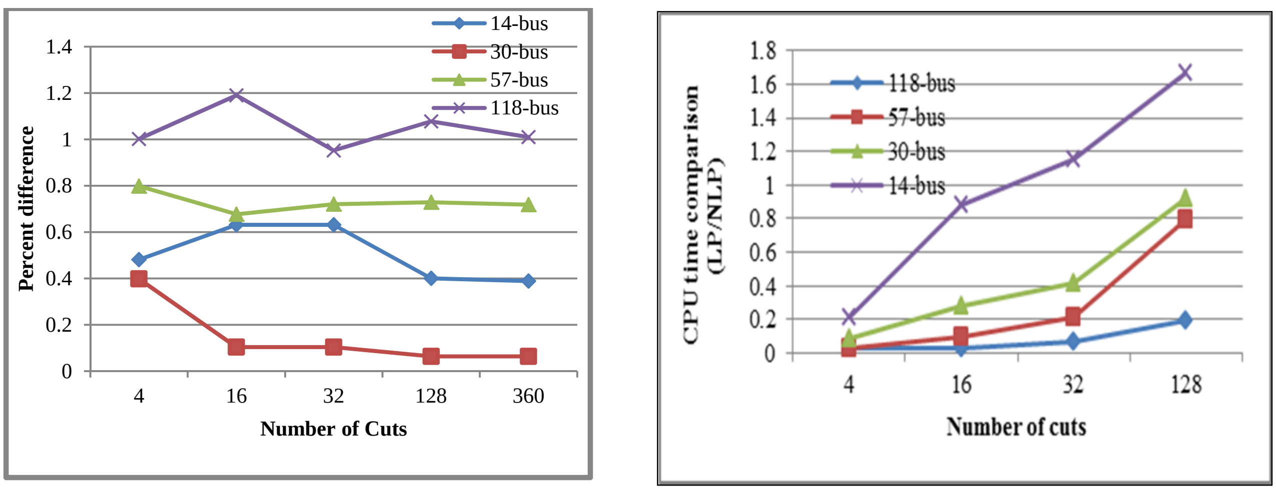

Figure 3. Objective Function Percent Difference and Execution Time Relative to the Nonlinear Solver for Loose Current Limit and Iterative Cuts

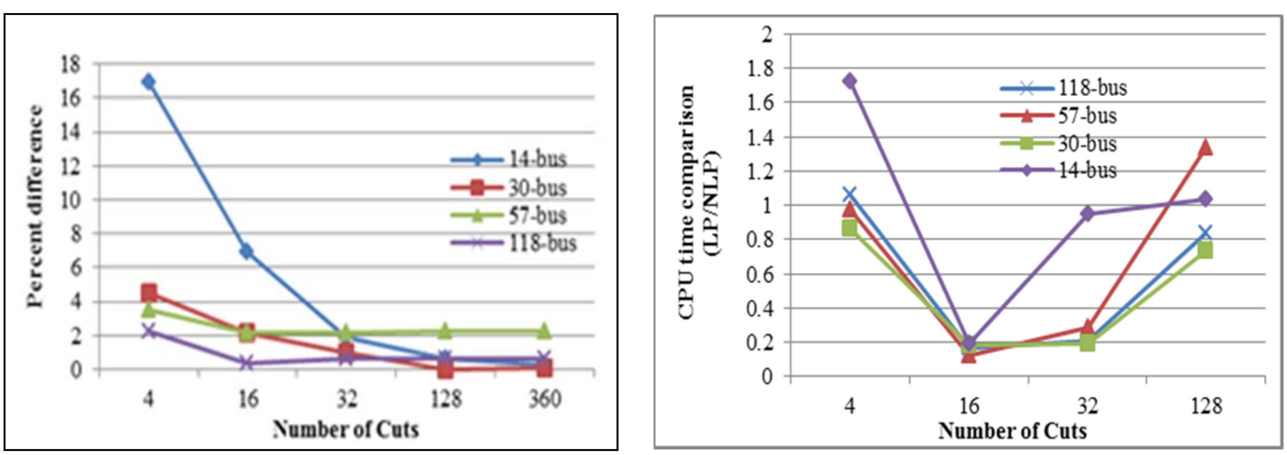

Figure 4. Objective Function Percent Difference and Execution Time Relative to the Nonlinear Solver for Tight Current Limit and No Iterative Cuts

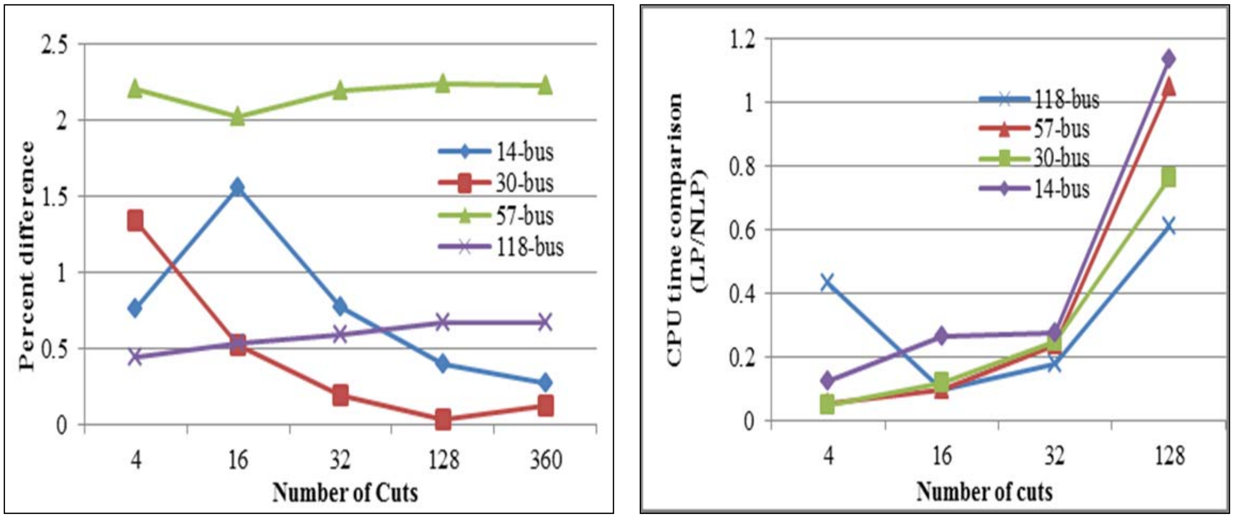

Figure 5. Objective Function Percent Difference and Execution Time Relative to the Nonlinear Solver for Tight Current Limit and Iterative Cuts

6. Conclusion

As the number of preprocessed constraints for each bus and line increases, the relative error decreases. For the problems tested, the results indicate that 16 to 32 constraints are the best number of preprocessed constraints in a tradeoff between accuracy and solution time. The marginal value of more than 32 and maybe 16 preprocessed constraints in this setting is negative. Nevertheless, the number of preprocessed constraints can be set based on the performance and requirements of the specific problem being solved. Using iterative cuts often results in faster convergence to a feasible solution. When solving without using iterative cuts, the solution is within 18% of the best-known nonlinear feasible solution; with iterative cuts, the solution is within 2.5% of the best-known nonlinear solution. At 16 or 32 preprocessed constraints, solution time is up to about 8 times faster than the nonlinear solver (IPOPT). This approach may be useful in solving optimal transmission topology and unit commitment problems because mixed-integer linear solvers are much faster than mixed-linear nonlinear solvers.

References

Mary B. Cain, Richard P. O'Neill, Anya Castillo, "History of Optimal Power Flow and Formulations," FERC Staff Technical Paper, December 2012, http://www.ferc.gov/industries/electric/indus-act/market-planning/opf-papers/acopf-1-history-formulation-testing.pdf

Florin Capitanescu, Jose Luis Martinez Ramos, Patrick Panciatici, Daniel Kirschen, Alejandro Marano Marcolini, Ludovic Platbrood, Louis Wehenkel, "State-of-the-art, challenges, and future trends in security constrained optimal power flow," *Electric Power Systems Research,* August 2011.

J. Carpentier, "Contribution á l'étude du dispatching économique," *Bulletin de la Société Française des Électriciens,* vol. 3, no. 8, pp. 431-447, 1962.

Anya Castillo and Richard P O'Neill, "Survey of Approaches to Solving the ACOPF",FERC Staff Technical Paper, March 2013a, http://www.ferc.gov/industries/electric/indus-act/market-planning/opf-papers/acopf-4-solution-techniques-survey.pdf

Anya Castillo and Richard P O'Neill, "Computational Performance of Solution Techniques Applied to the ACOPF", FERC Staff Technical Paper, March 2013b, http://www.ferc.gov/industries/electric/indus-act/market-planning/opf-papers/acopf-5-computational-testing.pdf

H. W. Dommel and W. F. Tinney, "Optimal Power Flow Solutions,", IEEE Transactions on Power Apparatus and Systems, vol.PAS-87, no.10, pp.1866-1876, Oct. 1968.

Frank and I. Steponavice, "Optimal Power Flow: a Bibligraphic Survey I Formulations and Deterministic Methods," *Energy Syst,* vol. 3, pp. 221-258, 2012.

M. Huneault and F. D. Galiana, , "A survey of the optimal power flow literature,", IEEE Transactions on Power Systems, vol.6, no.2, pp.762-770, May 1991

Paula A. Lipka, Richard P. O'Neill, and Shmuel Oren, "Developing Line Current magnitude Constraints for IEEE Test Problems", FERC Staff Technical Paper, April 2013. http://www.ferc.gov/industries/electric/indus-act/market-planning/opf-papers/acopf-7-line-constraints.pdf

J.A. Momoh, M. E. El-Hawary, and R. Adapa, "A Review of Selected Optimal Power Flow Literature to 1993. Part I: Nonlinear and Quadratic Programming Approaches", IEEE Trans. on Power Systems, Vol. 14(1): pp. 96-104, Feb. 1999.

Richard P O'Neill, Anya Castillo and Mary Cain, "The IV Formulation and Linear Approximations of the AC Optimal Power Flow Problem," FERC Staff Technical Paper, December 2012a, http://www.ferc.gov/industries/electric/indus-act/market-planning/opf-papers/acopf-2-iv-linearization.pdf

Richard P O'Neill, Anya Castillo and Mary Cain, "The Computational Testing of AC Optimal Power Flow Using the Current Voltage Formulations," FERC Staff Technical Paper, December 2012b, http://www.ferc.gov/industries/electric/indus-act/market-planning/opf-papers/acopf-3-iv-linearization-testing.pdf

T. Potluri and K. W. Hedman, "Impacts of topology control on the ACOPF," *IEEE Power and Energy Society General Meeting,* pp. 1-7, 2012.

R. E. Rosenthal and A. Brooke, "GAMS, a user's guide," *GAMS Development Corporation,* 2007.

E. Rothberg and R. Bixby, "Gurobi optimization," 2010.

Aaron Schecter and Richard P O'Neill, "Exploration of the ACOPF Feasible Region for the Standard IEEE Test Set", FERC Staff Technical Paper, February 2013, http://www.ferc.gov/industries/electric/indus-act/market-planning/opf-papers/acopf-6-test-problem-properties.pdf

B. Stott, O. Alsac and A. Monticelli, "DC power flow revisited," *IEEE Trans. Power Syst.,* vol. 24, no. 3, pp. 1290-1300, 2009.

Brian Stott and Ongun Alsaç, 'Basic Requirements for Real-Life Problems and Their Solutions", July 1, 2012, www.ieee.hr/_download/repository/Stott-Alsac-OPF-White-Paper.pdf

Waechter, Introduction to IPOPT, Carnegie Mellon University, 2007.

APPENDIX: NUMERICAL RESULTS

14-BUS SYSTEM

Table A1: Objective Function Values: 14-bus system, tight current constraint

	Number of cuts				
	4	16	32	128	360
LP-NoIterIVCut	89.2100	99.9100	105.3400	106.6800	107.0600
LP-IterIVCut	106.5500	105.6900	106.5300	106.9400	107.0700
NLP+LP Obj	107.3686	107.3686	107.3686	107.3686	107.3686

Table A2: Execution Time: 14-bus system, tight current constraint

	Number of cuts				
	4	16	32	128	360
LP-NoIterIVCut	1.940	0.220	1.070	1.170	2.660
LP-IterIVCut	0.140	0.300	0.310	1.280	2.580
NLP+LP Obj	1.125	1.125	1.125	1.125	1.125

Table A3: Objective Function Values: 14-bus system, loose current constraint

	Number of cuts				
	4	16	32	128	360
LP-NoIterIVCut	79.7700	85.8100	86.0500	86.1600	86.1700
LP-IterIVCut	86.0900	85.9600	85.9600	86.1600	86.1700
NLP+LP Obj	86.5062	86.5062	86.5062	86.5062	86.5062

Table A4: Execution Time: 14-bus system, loose current constraint

	Number of cuts				
	4	16	32	128	360
LP-NoIterIVCut	1.690	0.170	0.230	0.830	2.420
LP-IterIVCut	0.190	0.790	1.030	1.490	4.760
NLP+LP Obj	0.891	0.891	0.891	0.891	0.891

30-BUS SYSTEM

Table A5: Objective Function Values: 30-bus system, tight current limit

Number of cuts	4	16	32	128	360
LP-NoIterIVCut	5.8200	5.9600	6.0300	6.0900	6.1000
LP-IterIVCut	6.0100	6.0600	6.0800	6.0900	6.1000
NLP+LP Obj	6.0920	6.0920	6.0920	6.0920	6.0920

Table A6: Execution Time: 30-bus system, tight current limit

Number of cuts	4	16	32	128	360
LP-NoIterIVCut	4.540	0.950	0.990	3.870	10.520
LP-IterIVCut	0.270	0.630	1.310	4.010	10.090
NLP+LP Obj	5.234	5.234	5.234	5.234	5.234

Table A7: Objective Function Values: 30-bus system, loose current limit

Number of cuts	4	16	32	128	360
LP-NoIterIVCut	5.8200	5.9300	5.9700	5.9700	5.9700
LP-IterIVCut	5.9500	5.9800	5.9800	5.9700	5.9700
NLP+LP Obj	5.9738	5.9738	5.9738	5.9738	5.9738

Table 3: execution Time: 30-bus system, loose current limit

Number of cuts	4	16	32	128	360
LP-NoIterIVCut	16.870	1.490	1.420	3.310	10.600
LP-IterIVCut	0.480	1.630	2.400	5.340	15.330
NLP+LP Obj	5.812	5.812	5.812	5.812	5.812

57-BUS SYSTEM

Table A9: Objective Function Values: 57-bus system, tight current limit

Number of cuts	4	16	32	128	360
LP-NoIterIVCut	416.9117	422.9959	422.8063	422.4807	422.5419
LP-IterIVCut	422.6372	423.4306	422.7098	422.4812	422.5419
NLP+LP Obj	432.1900	432.1900	432.1900	432.1900	432.1900

Table A10: execution Time: 57-bus system, tight current limit

Number of cuts	4	16	32	128	360
LP-NoIterIVCut	19.709	2.436	5.780	27.088	87.331
LP-IterIVCut	1.127	2.041	4.832	21.268	59.018
NLP+LP Obj	20.281	20.281	20.281	20.281	20.281

Table A11: Objective Function Values: 57-bus system, loose current limit

Number of cuts	4	16	32	128	360
LP-NoIterIVCut	416.7944	424.7595	422.4737	422.3770	422.4237
LP-IterIVCut	422.0834	422.5992	422.4155	422.3798	422.4236
NLP+LP Obj	425.4805	425.4805	425.4805	425.4805	425.4805

Table A12: Execution Time: 57-bus system, loose current limit

Number of cuts	4	16	32	128	360
LP-NoIterIVCut	16.144	1.969	4.545	21.344	76.306
LP-IterIVCut	0.989	2.874	6.614	24.608	60.344
NLP+LP Obj	30.922	30.922	30.922	30.922	30.922

118-BUS SYSTEM

Table A13: Objective Function Values: 118-bus system, tight current limit

Number of cuts	4	16	32	128	360
LP-	1357.1281	1383.0689	1379.9237	1379.1194	1379.0062
LP-IterIVCut	1382.1567	1381.0145	1380.2231	1379.1220	1379.0067
NLP+LP Obj	1388.4251	1388.4251	1388.4251	1388.4251	1388.4251

Table A14: Execution Time: 118-bus system, tight current limit

Number of cuts	4	16	32	128	360
LP-NoIterIVCut	93.134	14.373	18.289	73.726	124.514
LP-IterIVCut	38.001	8.472	15.817	53.749	124.637
NLP+LP Obj	87.594	87.594	87.594	87.594	87.594

Table 4: Objective Function Values: 118-bus system, loose current limit

Number of cuts	4	16	32	128	360
LP-	1268.3334	1284.7513	1295.2132	1295.8839	1291.0350
LP-IterIVCut	1287.1712	1287.5420	1298.0719	1291.0000	1296.2755
NLP+LP Obj	1315.4988	1315.4988	1315.4988	1315.4988	1315.4988

Table 5: Execution Time: 118-bus system, loose current limit

Number of cuts	4	16	32	128	360
LP-NoIterIVCut	68.232	259.395	446.980	1885.862	3869.237
LP-IterIVCut	130.440	256.572	438.003	1497.221	3983.677
NLP+LP Obj	70.719	70.719	70.719	70.719	70.719